Chapter 2

Qualitative description of the technique.

The intensity of the light scattered from a spatially disordered sample has a speckled appearance, the speckles being generated by the random interference of the scattered elementary spherical waves. While the study of the one point intensity time correlations has proven very useful, and it has generated the technique of Intensity Fluctuation Spectroscopy (IFS) [5], the measurement of the two point, equal time, intensity space correlation function, that is the size and the shape of the speckles, does not provide any useful information. Indeed the Van Cittert and Zernike theorem states that the *far field* space correlation function depends only on the intensity distribution of the scattering volume, and in no way depends on the physical properties of the sample.

In this chapter we will present qualitative elements showing that for fluctuations the size of the wavelength of light or larger, in the *near field* we obtain a speckle field, that is, a gaussian field; moreover its statistics is directly related to the scattered intensity distribution. We will derive the working formulas for three tecniques, hOmodyne Near Field Speckles (ONFS), hEterodyne NFS (ENFS) and Schlieren-like NFS (SNFS); analogies with the IFS will be pointed out. Advantages with respect to the more conventional Small Angle Light Scattering (SALS) technique will be discussed.

First of all, we will describe ONFS setup; many considerations hold also for ENFS and SNFS. The experimental set-up is very unorthodox, with respect to a conventional SALS device. It consists of a wide laser beam and of a Charge Coupled Device (CCD) detector positioned so to be flooded with light coming from any scattering direction the system can scatter at.

The Van Cittert and Zernike theorem states that the field correlation function is [6]:

$$C_E(\Delta x, \Delta y) = \langle E\,(x,y)\,E^*(x+\Delta x, y+\Delta y)\rangle = \int\int I(\xi,\eta) exp\left[i\frac{2\pi}{\lambda z}\,(\xi\Delta x + \eta\Delta y)\right] d\xi d\eta \quad (2.1)$$

where $E(x,y)$ is the field in the observation plane $x-y$, λ is the wavelength and $I(\xi,\eta)$ is the actual intensity distribution of the source in the plane $\xi-\eta$ at a distance z from the observation plane. The theorem holds for sources consisting of point emitters, like atoms. The intensity correlation function $C_I(\Delta x,\Delta y) = \langle I(x,y)\, I(x+\Delta x, y+\Delta y)\rangle$ is then derived by applying the so called Siegert relation [7]:

$$C_I(\Delta x,\Delta y) = \langle I\rangle^2 + |C_E(\Delta x,\Delta y)|^2 \tag{2.2}$$

Equations (2.1) and (2.2) specify that the intensity correlation function is related to the space Fourier transform of the source. In practice, this implies that a source of size D will generate speckles of size $\frac{\lambda}{D}z$ on a screen positioned at a distance z [7].

We will start introducing simple euristic arguments and crude evaluations for the near field speckles of the scattered light. Let us consider the case of a large beam diameter D, impinging onto a sample of particles of diameter d larger than the wavelength of light: see Figure 2.1(a). Most of the power will be scattered in a forward lobe of angular width $\Theta \approx \frac{\lambda}{d}$. Let us consider a small area S, for example a multi-element sensor array, in the immediate vicinity of the scattering volume: see Figure 2.1(b). Let us assume that we can ignore the transmitted beam: we will take care of this problem later on. Although the sample is illuminated over the entire surface of diameter D, the light falling onto the sensing area will come only from a smaller area of diameter D^* . In fact the brightness of the scattering volume will change as a function of the observation angle in a way that mirrors the scattered intensity distribution. Consequently, for the sensing area, the source region from which light is drawn is a circle with a diameter $D^* = \frac{\lambda}{d}z$, z being the distance of the sensing area from the scattering surface; source regions outside do not contribute appreciably. We say that the near field condition is met if $D^* \ll D$. One can then immediately estimate the size of the speckles $d_{sp} = \frac{\lambda}{D^*}z \approx d$, a remarkable result in many respects! The speckles have the size of the particle diameter, and this value does not depend on the distance z from the sample, provided the near field condition $D^* \ll D$. This has to be compared with far field speckles, whose diameter scales linearly with the distance from the source. Also notice that the actual sample thickness does not matter, provided that the near field condition is met, and that the speckle size does not depend on the light wavelength, an unexpected feature for an interference pattern.

Notice that all the above applies under conditions that are more stringent than the usual "near field" condition [8] for a source of size D , namely $\frac{\lambda z}{D^2} \ll 1$. In the present case the condition is $D^* \ll D$ which implies $\frac{\lambda z}{Dd} \ll 1$.

To put things in a more quantitative way, we will determine the near field intensity correlation by first re-writing the Van Cittert and Zernike theorem in a more appropriate form. We notice that Eq. (2.1) may be rewritten in the

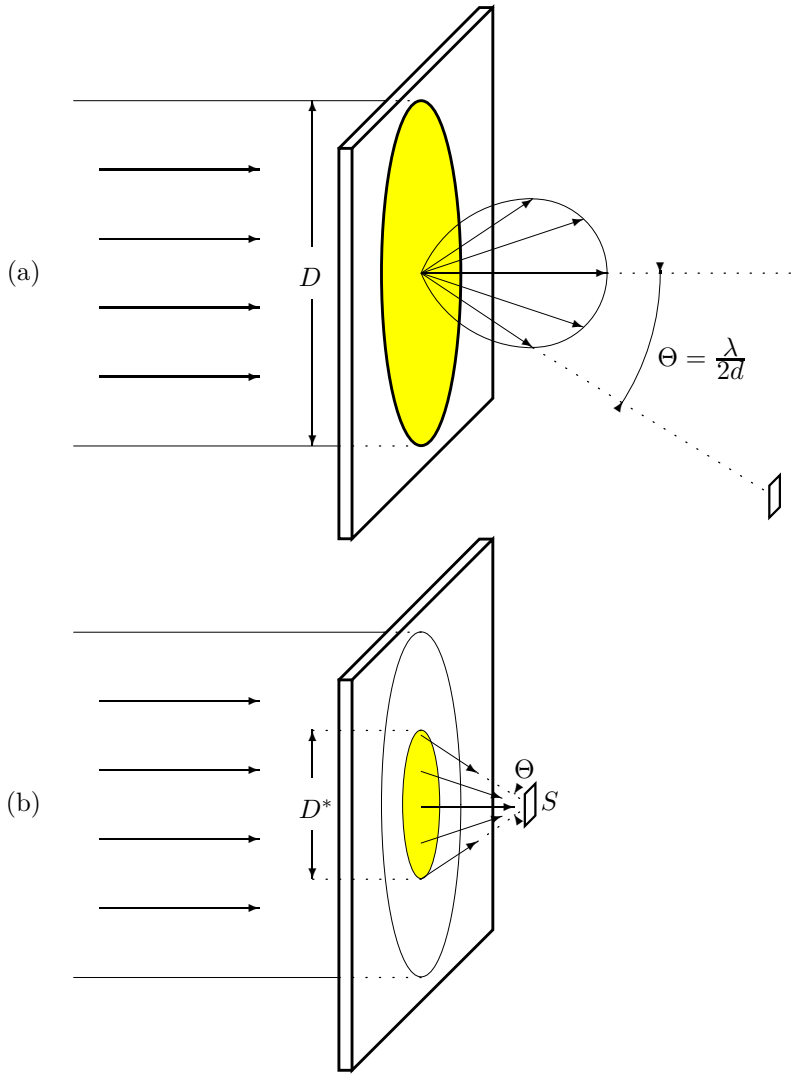

Figure 2.1: (a) Small angle scattering. A beam of diameter D impinges onto a sample composed of particles of diameter d. Any zone within D will scatter light into a lobe of angular width $\Theta = \lambda/d$ (the length of arrows indicates scattered intensity). (b) Same sample, as in part (a). A sensor S close enough to the sample will draw light only from a zone of radius $D^* < D$. Regions outside, even if illuminated by the main beam, do not feed light to S. Notice that again $\Theta = \lambda/d$.

following way:

$$C_E(\vec{r}) = \int I(\vec{q})\, e^{i\vec{q}\cdot\vec{r}} \mathrm{d}\vec{q}, \tag{2.3}$$

where $\vec{r} = (\Delta x, \Delta y)$, and $\vec{q}$ is a vector whose components are $q_x = \frac{2\pi}{\lambda z}\xi$ and $q_y = \frac{2\pi}{\lambda z}\eta$, which equals the scattering wave vector for small scattering angles.

Equation (2.3) is only a different way of writing Eq. (2.1), and $I(\vec{q})$ is the intensity distribution of the source as seen from the observation plane as a function of the scaled angles $(2\pi/\lambda)(\xi/z)$, and $(2\pi/\lambda)(\eta/z)$. As discussed in the introductory remarks, in the very near field $I(\vec{q})$ equals the scattered intensity distribution, which is proportional to the Fourier transform of the sample density correlation function $g(\vec{r}) = \langle \delta l(\vec{r})\, \delta l(0) \rangle$, where δl is the local fluctuation of the particle number density, integrated over the light path. Then, from Eq. (2.2), it follows that:

$$C_I(\vec{r}) = \langle I \rangle^2 \left[1 + |g(\vec{r})|^2 \right]. \tag{2.4}$$

We would like to point out that Eq. (2.4) closely duplicates the well known relation that holds for the IFS $< I(0)I(t) >=< I >^2 [1 + |g(t)|^2]$, where $g(t)$ is the time correlation function (see for example [9]). It should be noted that for some scatterers the Rayleigh Gans approximation is invalid, for example for larger spheres where the Mie theory applies, and therefore the pair correlation function $g(r)$ cannot be extracted from the scattered light. It remains true however that even in those cases the correlation method permits the determination of the scattered intensity distribution $I(q)$, by using the relation:

$$C_I(r) = \langle I \rangle^2 \left[1 + \left| \int I(q)\, e^{i\vec{q}\cdot\vec{r}} \mathrm{d}\vec{q} \right|^2 \right]. \tag{2.5}$$

To determine the spatial intensity correlation of Eq. (2.4), one must first obtain experimentally the instantaneous intensity distribution of the near field scattered light. In order to evaluate the intensity correlation function with reasonable statistical accuracy it is also imperative to gather intensity distributions over a substantial number of points. To this end a CCD is ideal, the number of pixel being larger than 10^5. As we shall see, it actually turns out that one frame is enough for a fair acquisition of the correlation function.

In a previous work [1], some measurements have been performed on a scattering model, an opaque metallic screens with pinholes of 140 and 300 microns chemically etched in random positions. The surface fraction occupied by the pinholes was around 10% and 20% respectively. Experimentally this greatly simplifies the problem, since the scattered field is stationary and also there is no transmitted beam. We call this configuration hOmodyne Near Field Speckles, since the signal is given by the interference of different scattered beams. Being a two dimensional sample, the scattered intensity was simply related to the correlation function of the transparency function $T(x, y)$ with $T = 1$ inside

the pinholes and zero outside [6]. A Helium Neon parallel beam with diameter ($\frac{1}{e^2}$ points) $D = 15$mm was sent onto the samples, and the speckle field was recorded with a CCD at various distances $z = 50$cm, $z = 75$cm and $z = 100$cm [1]. The corresponding values for D^* ranged from 1mm to 4.3mm so that the very near field condition was always met. The rather large dimension of the pinholes was chosen so that the speckles were appreciably larger than the CCD pixel size (typically 9μm). For each type of pinholes, the measurements performed at the three distances showed minute differences. The results are shown in Fig 2.2, where the data are compared with the correlation functions of digitised images of the set of pinholes on the metallic screen [2]. Since in this case the sample is two-dimensional, $g(\vec{r})$ is the correlation function of $T(\vec{x})$. The width and shape of the main peak are fairly well reproduced, in spite of the limited number of frames used (four frames on statistically equivalent samples for each type of pinholes).

While the data obtained with the screens prove that near field speckles do mirror the properties of the scatterers, we feel that to assess the desirability of the technique for realistic applications (for example in colloid physics) measurements had to be taken with particle solutions down in the micron range. In order to do this, three problems had to be solved. The speckles in the near field close to the cell have dimensions around one micron and therefore are too small for the available CCD pixel size. Also, one must dispose of the transmitted beam. Finally, the speckle intensity distribution must be frozen at a given instant.

The first two problems have been solved with the simple optical arrangement shown in Fig. 2.3. A wide parallel beam is sent onto the sample, placed against a large aperture lens of focal length f. A wire is stretched in the focal plane to intercept the main beam. The CCD is placed a distance q away from the lens. The system magnifies the speckle size by a factor $M = (q - f)/f > 1$, and the scattering angles are decreased accordingly. It is illuminating to point out that the technique can be considered as a scaled down version of the classical Hanbury Brown and Twiss [10] experiment where the star intensity distribution is mimicked by the scattered light intensity patch in the focal plane, and the ground based intensity correlation are the CCD intensity correlations. The unavoidable presence of the lens and its finite aperture introduces some complication with respect to the lensless arrangement used for the pinholes. In a previous work [1], the poor numerical aperture of the lens introduced a non-uniform transfer function, which had to be evaluated by measuring a known sample. In the present work, care has been taken in order to avoid such problems.

When the scattered speckles are observed with the CCD in real time, one

[1] For very large objects the near field is not really near, since one must let the diffraction figures from various objects interfere. This leads to the additional condition $D^* = \frac{\lambda}{d} z \gg \delta$, where δ is the typical distance between scatterers.

[2] Experimental correlation functions shown in figure are calculated according to the following procedure. First, the Fast Fourier Transform of the intensity distribution is calculated. Then the result is squared. The auto-correlation is then obtained by anti-transforming the power spectrum.

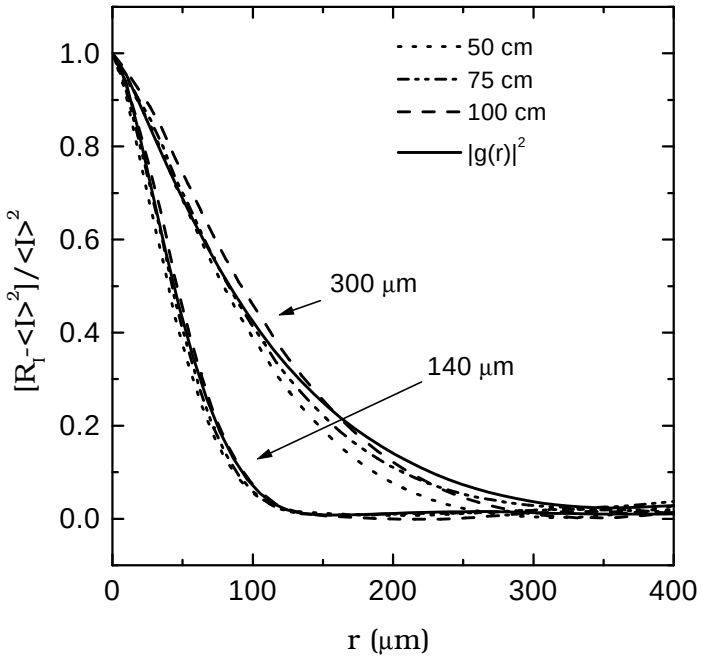

Figure 2.2: Measured intensity auto-correlations as a function of displacement r for two sets of randomly positioned pinholes, of 140μm and 300μm in diameter. For both the samples, measurements at three distances are reported, together with $|g(r)|^2$, calculated from the digitized images of the two samples.

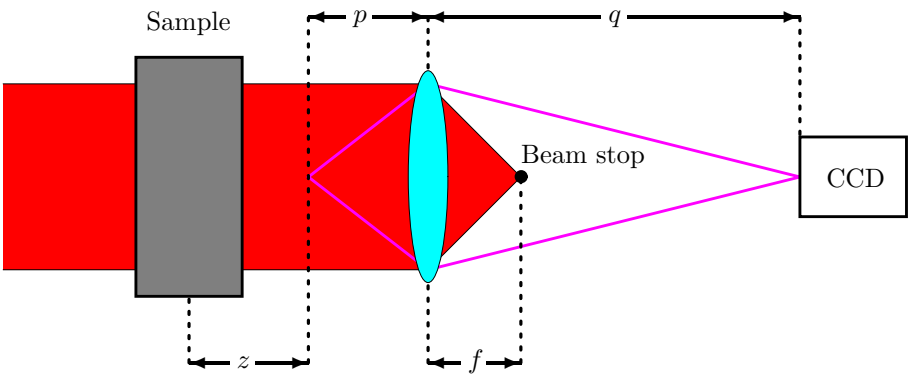

Figure 2.3: Optical layout for ONFS. The main transmitted beam is blocked by a stop in the focal plane. Almost all the scattered light is sent to the CCD.

notices quite vividly that the speckle size changes as the size of the scatterers is changed. Also, for a given sample the speckles boil with the same time constant on the whole screen, the time constant getting larger for samples with larger diameter particles. With regard to the third problem mentioned above, these observations also indicate that even with a conventional CCD and a small power He-Ne laser there is no problem in getting instantaneous pattern distributions. Indeed even for the smallest particles that can be studied with present experimental set-up, with diameters down to 1μm, and assuming diffusive motion, the shortest time constant associated to the smallest scattering wavevector yields $\tau_{min} = 0.125$s, a time long compared with the shortest frame exposure available with standard frame grabbers, typically 1/16000s.

Let us compare the Near Field Speckles technique with the more traditional Small Angle Light Scattering. The essential feature of a scattering layout [11, 12] is that the light scattered at a given angle hits the sensors along a circle of given diameter around the optical axis. We believe that the correlation method of NFS offers some distinct advantages over the scattering technique. First, there is no need for accurate positioning of the CCD, that can be rather casually placed at a distance z from the focal plane (see Fig. 2.3). At variance, in SALS one has to know the precise relation between pixels and scattering angles and this is troublesome when the distance z is changed to select a new particle diameter instrumental range. Also, and more important, SALS is plagued by stray light. To mitigate its effects, one has to rely on blank measurements to be subtracted from raw scattering data. The trouble is that stray light is worst at smaller angles, where the sensing elements are necessarily in small number and crowded close to the optical axis. With the present technique, on the contrary, all the pixels are used in calculating the correlation function for any value of the displacement r and this allows more accurate stray light subtraction; the

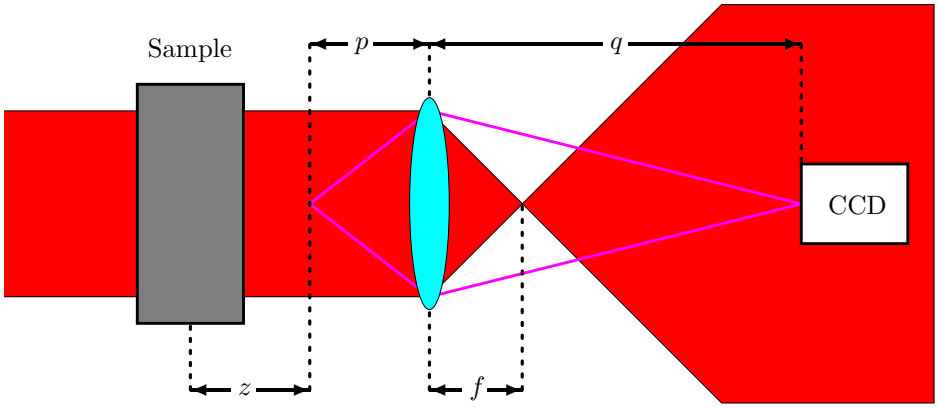

Figure 2.4: Optical layout for ENFS. The main transmitted beam is not blocked by the stop in the focal plane. Both the scattered and the transmitted beams are sent to the CCD.

algorithms to subtract the stray light will be described in Chapter 5.

The results of the measurements on some colloid samples are presented in Chapter 7. The ONFS technique in the present form has only one tight requirement, namely the clean disposal of the transmitted beam that requires accurate focusing and a proper diffraction limited beam stop. It is both conceptually and in practice very simple, and it capitalizes on the high statistical accuracy permitted by the large number of pixels of a CCD and by the good handling capabilities of PCs.

It became soon appearent that the main problem with ONFS comes from the poor statistical quality of the calculated $I(q)$. In Chapter 7 we will show that the statistical quality increases only as the fourth root of the number of processed images. We experimented a different optical setup (ENFS), drawn in Fig. 2.4. In ENFS, there's no beam stop: the main beam is let interfere with the scattered light. This is basically an heterodyne version of NFS, thus we call it hEterodyne Near Field Speckles (ENFS).

Basically, ONFS data processing consists in evaluating the field correlation function $C_E(\vec{r})$ by using Siegert relation (2.2), then evaluating $I(q)$ by applying the inverse Fourier transform to (2.3). In ENFS, we measure the interference between the speckle field of ONFS with the much more intense transmitted beam. We directly measure a quantity linearly related to the field. The intensity correlation function of an ENFS image equals $C_E(\vec{r})$, provided that all the conditions needed by ONFS are met, that is, if the field is circular gaussian. We thus obtain $C_E(\vec{r})$ without the data inversion needed to apply Siegert relation, and this greatly enhances the statistical accuracy of the results.

In Chapter 7 we show a comparison between data taken with ONFS and ENFS; data taken with ENFS are evidently much less noisy. The quality is comparable with the SALS one. This good quality allowed to try a Mie-based

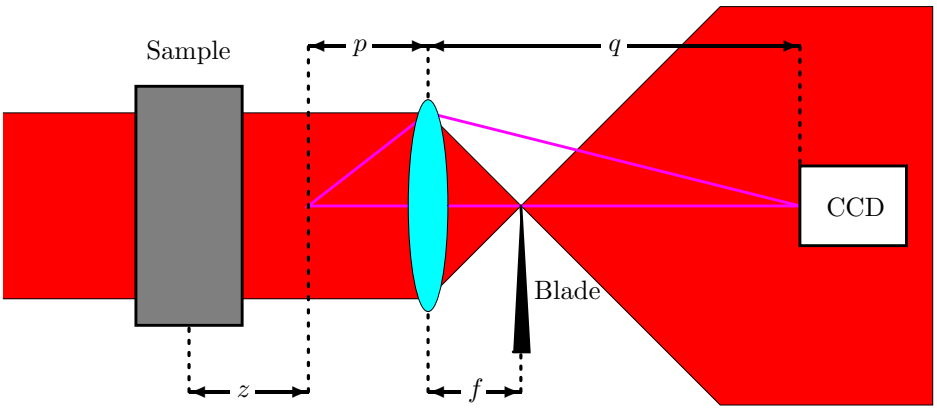

Figure 2.5: Optical layout for SNFS. Part of the transmitted beam is blocked by a blade in the focal plane, along with half of the scattered light. Only one half of the scattered light is sent to the CCD, along with a part of the transmitted beam.

inversion algorithm, to obtain an histogram of the distribution of the diameters of some colloidal samples; the measurements are shown in Chapter 8.

Both ONFS and ENFS are quite sample wasting techniques. They require a sample much bigger than the statistical quality needs. For example, consider a non-equilibrium fluctuation measurement in a free diffusion experiment [13]. The biggest fluctuations we want to measure are about 0.5mm. A good statistical sample should be so big to contain some hundred of the biggest fluctuations: it can be a square with a 5mm side. This is enough for SALS, but not for ONFS nor ENFS. In Chapt. 3 we will show that, if we want to cover two decades in wavevectors, we must use a sample with side $5\text{mm} \cdot 10^2$. To cover two decades, we need a half a meter wide cell, while with SALS we can work with a half a centimeter wide cell! This is not a difficulty for particle sizing applications, but can become a serious problem when we want to analyze many lenghtscales, since NFS is particularly suited for big objects. This problem is essentially due to the fact that big objects need long values of z in order that their scattered field is gaussian; on the other hand, we need a big sample, so that the sensor collect the light scattered at high angles by small particles. This fact is quite unusual, since in general big objects are good subjects for classical microscopy techniques. The difficulty can be easily circumvented, introducing a new instrumental setup, called SNFS: see Fig. 2.5. This setup closely mirrors the Schlieren setup: a blade stops half focused trasmitted beam, along with one half of the scattered light. In the case of a two dimensional sample, we can create an image of it on the CCD sensor, as in classical Schlieren imaging technique. But in the case of three dimensional samples, the smaller objects create a speckle field, while the bigger ones are completely resolved: this technique passes continuously from the deterministic image formation of the big objects,

like in microscopy techniques, to the analysis of stochastical interference patterns of NFS, without the need to know at what lengthscale the passage takes place. We will show that SNFS doesn't require any condition on the position of the focal plane: it can be made as near to the sample as we need; moreover, the dimensions of the sample can be quite small, as in SALS.

SNFS requires an additional element with respect to ENFS, the blade, but it allows easy measurements on many lengthscales, on big objects. We used such a technique to measure the power spectrum of non-equilibrium fluctuations in a free diffusion experiment, described in Chapter 9, thus showing that this technique can be applied to researches in fundamental physics.